Studies on the Growth, Luminescence, Electrical, Mechanical properties and Surface Topography of Bisthiourea Cadmium Acetate

V.Rajendran, J.Uma*
Department of Physics, Presidency College, Chennai – 600 005, Tamilnadu, India
Tel. : +91 44 26561236.
*umakanarayana2009@gmail.com

ABSTRACT

Nonlinear optical material Bisthiourea cadmium acetate (BTCA) was grown by slow evaporation solution growth technique. The morphology of the grown crystal was studied to identify the prominent planes of growth. The powder diffraction peaks indicates that the grown crystal is highly crystalline in nature. The photoluminescence studies reveal the crystal show blue emission with the peak at 481nm. The dielectric constant and dielectric loss was measured over the frequency range of 50Hz–5MHz. Dielectric constant and dielectric loss decreases at higher frequencies for various temperatures that ensure that the crystal is a potential material for NLO applications. The mechanical stability was studied by Vickers microhardness test. The hardness increases with the increasing load indicates the Reverse Indentation Size Effect (RISE). Elastic stiffness constant (C_{11}) indicates that the binding forces between the ions are strong. The surface topography of the crystal was studied using scanning electron microscopy (SEM) and atomic force microscopy (AFM) respectively. The surface roughness parameter from AFM study shows that the grown crystal possesses a smooth and flat surface.

Keywords:

Photoluminiscence ,SEM, AFM, dielectric property, Mechanical Properties.

1. Introduction

In search of new frequency conversion materials, recent interest are in semi-organic materials due to their large nonlinearity, high resistance, large induced damage, low angular

sensitivity and good mechanical hardness [1-3]. Thiourea in combination with metal complexes forms semi-organic compound gives a low cutoff wavelength and it is applicable for high frequency conversion. To introduce the asymmetric conjugated organic molecules into inorganic distorted polyhedra, several thiourea complexes were synthesized and screened for their second harmonic generation (SHG) efficiencies[4].Transition materials (Zn, Cd, and Hg) have high conversion efficiency because the metal center is engaged in π-bonding with the organic ligating groups [5,6]. Some of the earlier reported thiourea based semiorganic crystals are Zinc Thiourea Chloride [7], Zinc Thiourea Sulphate[8], Bisthiourea Cadmium Chloride[9], Bisthiourea zinc acetate [10], Bisthiourea cadmium formate[11]. In this series, large single crystal of Bisthiourea cadmium acetate (BTCA) of size 55 x 45 x 1mm^3 was grown by slow evaporation method by the authors [12]. In the present work, growth morphology, powder XRD, Photoluminiscence, dielectric studies, Microhardness studies, SEM and AFM analysis were studied and reported.

2 MATERIALS AND METHODS

2.1 SYNTHESIS AND CRYSTAL GROWTH

The BTCA crystal was synthesized according to the procedure described earlier [12]. The purity of the synthesized salt was improved by the repeated recrystallization process.

2.2 Solubility

The solubility studies of the synthesized BTCA were determined for ethanol and water at five different temperatures. The crystals are dissolved in the solvents separately taken in an air tight container, maintained at a constant temperature with continuous stirring. After attaining the saturation, the equilibrium concentration of the solute is analyzed gravimetrically. Figure 1 shows the solubility curve of the BTCA in water and ethanol. From the graph, it is found that the solubility of the BTCA increases with temperature and possesses positive gradient of

solubility with good solubility in water.

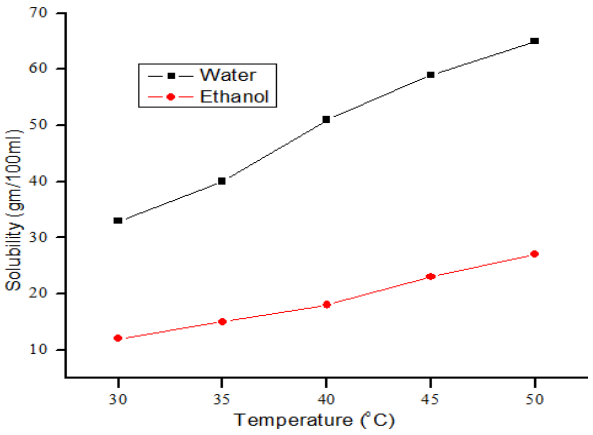

Figure 1 Solubility curve of BTCA

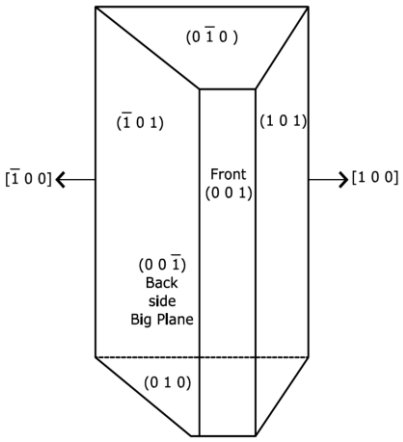

Figure 2 Morphology of BTCA

3 RESULTS AND DISCUSSION

3.1 Morphology and Powder X-ray Diffraction studies

The morphology of the grown crystal was done using Enraf Nonius CAD4 MV31 diffractometer and is shown in Figure 2. It was observed that the growth along the 'b' axis is much higher than that of 'a' and 'c' axes. The prominent planes are (101),(001),(010) $(0\bar{1}0), (\bar{1}01)$ and $(00\bar{1})$. The plane $(00\bar{1})$ is the most prominent plane and the other well-developed planes are $(\bar{1}01)$,$(0\bar{1}0)$, (101) and (010) that dominates the crystal morphology.

Powder X-ray diffraction pattern was recorded using CuKα (K = 1.5418 Å) radiation over the range of 10-70° at a scanning rate of 1°/minute. A graph is plotted between the intensity of the diffracted beam and the angle of diffraction. The diffracted peaks were indexed as shown in Figure 3 which confirms the perfection of good quality single crystal.

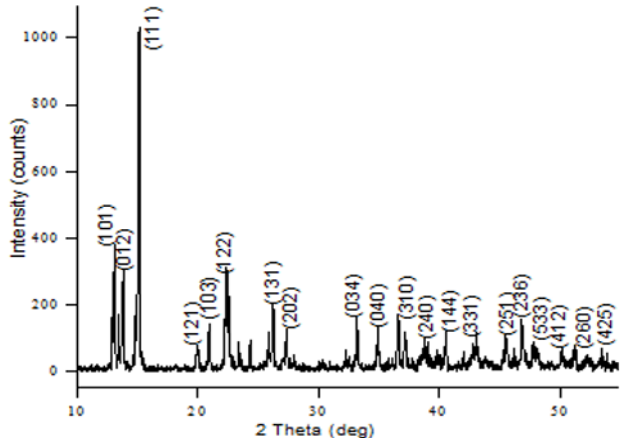

Figure 3 Powder X-Ray Diffraction of BTCA

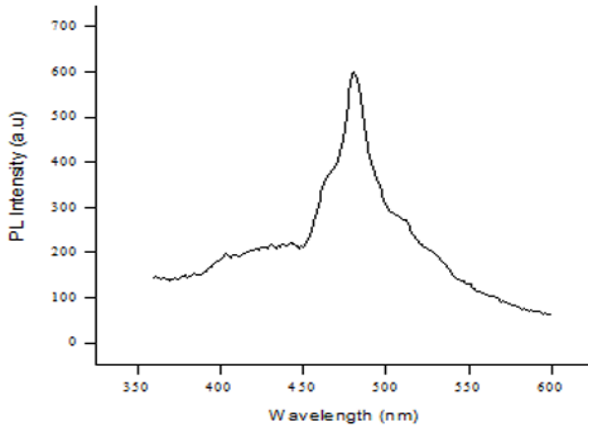

Figure 4 PL Spectrum of BTCA

3.2 Photoluminescence Studies

Photoluminescence (PL) is a characterization tool for analyzing the material, estimating the purity and crystalline quality of the sample. The steady state photoluminescence (PL) spectra of the grown crystals are recorded using an Edinburgh Luminescence Spectrometer (Model: F900), equipped with a Xe 900, xenon arc lamp. Figure 4 shows the PL spectrum of the BTCA crystal recorded using luminescence spectrometer operating at ambient conditions with the corresponding excitation wavelength of 320 nm. In the spectrum, a maximum peak was observed at 481 nm, which is the blue region in the electromagnetic spectrum. The single broad emission confirms the structural perfection of the grown crystal. This shows that BTCA crystal is a good candidate for absorption of ultraviolet light and emission of light in blue region. The strong broad PL emission in the blue region confirms the suitability of BTCA crystal for optoelectronic and luminescence devices[13].

3.3 DIELECTRIC STUDIES

The dielectric studies was measured using HIOKI 3532-50 LCR meter for the sample of size 5.30×3.28×2.41 mm^3 and was coated with silver paste to obtain good Ohmic contact. The experiment was carried out in the frequency range of 50Hz–5MHz at different temperatures

(313,333,353 and 373 K).The variation of dielectric constant (ε_r), dielectric loss (tanδ) and AC conductivity (σ_{ac}) were measured as a function of frequency at different temperatures.

Dielectric constant and Dielectric loss were calculated using the Equation (1) and (2) respectively

$$\varepsilon_r = \frac{Cd}{\varepsilon_o A} \quad (1)$$

$$\tan \delta = \varepsilon_r D \quad (2)$$

where *C* is the capacitance, d is the thickness of the sample, $\varepsilon_o = 8.854 \times 10^{-12} Fm^{-1}$ is the permittivity of free space, A is the area of cross section and D is the dissipation factor. Figure 5 and 6 shows the variation of dielectric constant and dielectric loss with respect to varying frequencies at different temperatures. It was found that the dielectric constant and dielectric loss decrease exponentially with the increase of frequency at all temperatures. The high values of ε_r and tan δ at low frequencies are due to the presence of space charge, orientational, ionic and electronic polarizations. As the frequency increases, the space charge polarization cannot sustain and comply with the external field and hence the polarization decreases[14,15].The low value of dielectric loss at high frequencies revealed that the high optical quality of the crystal with less electrically active defects is a desirable property for NLO applications [16,17].

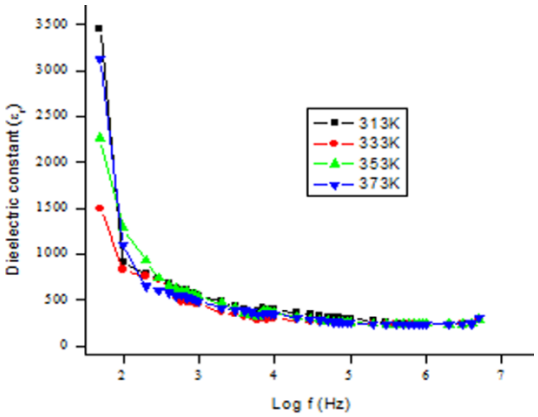

Figure 5 Dielectric constant vs log frequency

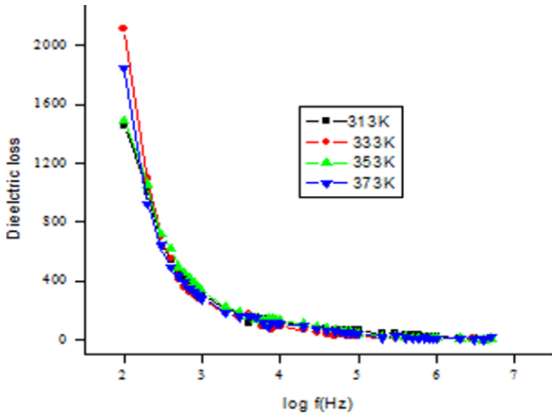

Figure 6 Dielectric loss vs log frequency

The AC conductivity (σ_{ac}) of the crystal is calculated using the Equation (3)

$$\sigma_{ac} = \omega\, \varepsilon_o \varepsilon_r \tan\delta \qquad (3)$$

The Figure 7 shows the variation of ac conductivity with frequencies for different temperatures. The increase in ac conductivity at higher frequency is due to the reduction in the interfacial polarization [18]. At low temperatures the conductivity is less due to trapping of charge carriers at defect sites. As temperature increases, more defects are created by thermal activation and the conductivity increases. The high value of conductivity at higher frequencies for all the measured temperatures indicates the dielectric breakdown of the material [19].

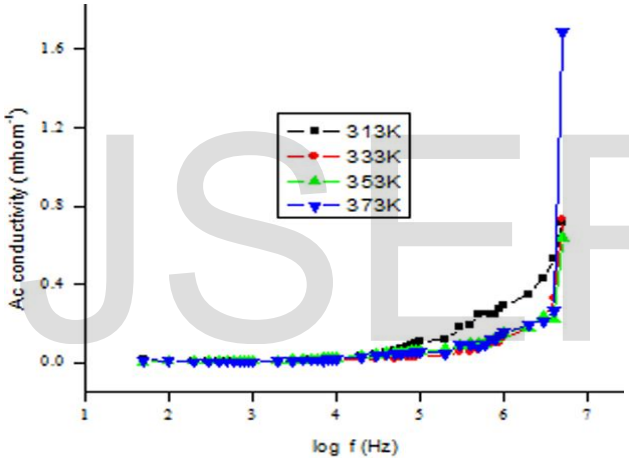

Figure 7 Log frequency versus AC conductivity

3.4 MICROHARDNESS STUDIES

The mechanical property was studied using SHIMADZU HMV 2T Vickers hardness tester, fitted with a Vickers's diamond pyramidal indenter. The hardness values (H_v) were calculated from the Equation (4)

$$H_v = \frac{1.8544\mathrm{P}}{d^2} \qquad \mathrm{Kgmm^{-2}} \qquad (4)$$

where P is the applied load and *d* is the mean diagonal length of the indentation. It is observed that the H_v increases with the increasing of load which indicates the Reverse Indentation Size Effect (RISE) (Figure 8) [20,21]. The RISE can be related to energy loss owing to the cracking

of the specimen during indentation [22]. An increase in the mechanical strength will have significant effect on NLO device fabrication and processing [23].

The Meyer's law [24] relates to load and size of indentation as

$$P = ad^n$$

$$\log P = \log a + n\log d \quad (5)$$

Here, 'a' is a constant for a given material. The work hardening coefficient 'n' was determined from the slope of the plot of log d versus log P (Figure 9) by fitting data using least-squares fit method and the value of n was found to be 4.43. In general, the working hardening coefficient (n) should lie between 1 and1.6 for hard materials and it is n> 1.6 for soft materials [25,26]. The 'n' value of BTCA crystal is 4.43 and hence it belongs to soft material category.

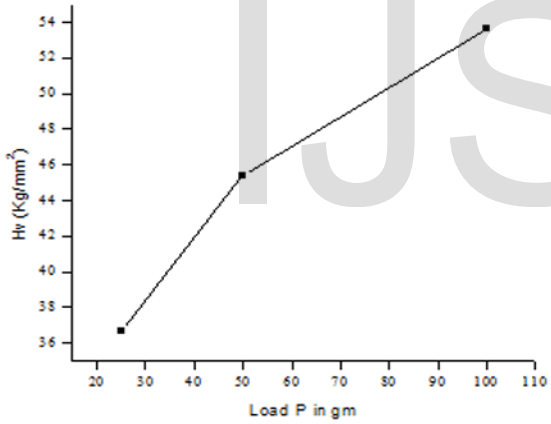

Figure 8 Vickers hardness number vs load

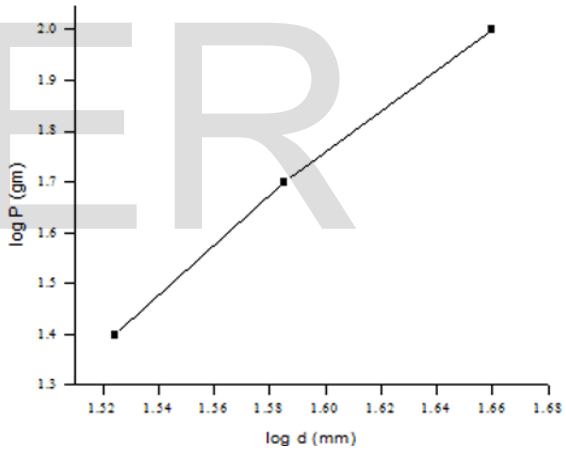

Figure 9 Plot of log d vs log P

Using Wooster's empirical formula [27] $C_{11}=Hv^{7/4}$, the elastic stiffness constant (C_{11}) of BTCA was calculated for different loads which indicates the binding forces between the ions. The calculated values of C_{11} for different loads for BTCA crystal are shown in Table 1 which indicates that the binding forces between the ions in BTCA are strong. The yield strength (σ_v) can be calculated from the microhardness value for n >2 using the Equation (6) [28].

$$\sigma_v = \frac{H_v}{2.9}[1 - (n-2)]\left[\frac{12.5(n-2)}{[1-(n-2)]}\right]^{(n-2)} \quad (6)$$

For BTCA crystal the yield strength was calculated for various loads as shown in Table 1.

Table 1: C_{11} and σ_v for various loads of BTCA crystal

S.No	Load (gm)	C_{11} ($x10^{12}$ Pa)	σ_v ($x10^{10}$ Pa)
1	25	17.2635	3.0343
2	50	25.1101	3.7587
3	100	33.5767	4.4376

3.5 SEM ANALYSIS

SEM analysis was carried out using Quanta 200 FEG scanning electron microscope and gold coating was done before subjecting crystal surface to electron beam. The SEM images of BTCA with different magnification are shown in Figure 10. It exhibit sphere like tiny crystals that are merged with one another. These basic units are arranged in different layers, which is a clear evidence for the stacking during crystal growth [29].

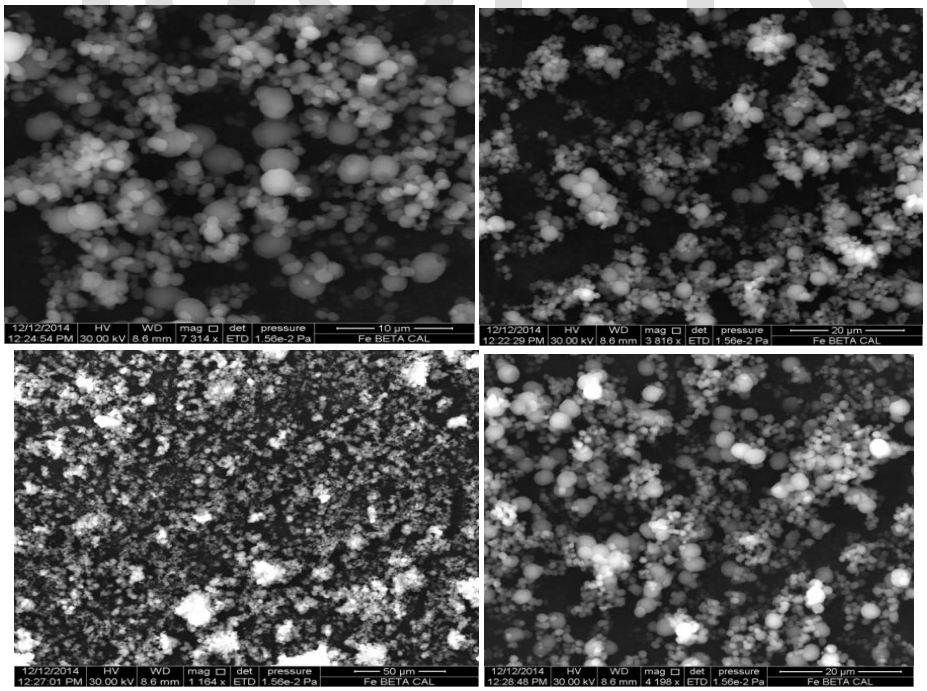

Figure 10 SEM images of BTCA single crystal

3.5 AFM ANALYSIS

The AFM analysis of the grown crystal was done using NTEGRA PRIMA, NTDMT, in semi contact mode. Figure 11 shows the AFM image of BTCA crystal. The images reveal that the surface of BTCA contains number of peaks and valleys. A large number of peaks and valleys in an image significantly affect the average roughness parameter values but for BTCA crystal the parameters S_a=17.24 nm and S_q=23.55 nm are very low that indicates that the crystal possesses almost smooth surface. [30]. The surface parameters of BTCA crystal are shown in Table 2. The surface skewness (S_{sk}) is an important parameter which is the measure of surface sharpness. if the height distribution is asymmetrical, the surface has more peaks than valleys, the Skewness moment is positive, and if the surface is more planar and the valleys are predominant then the Skewness is negative[30]. The surface skewness value of BTCA is negative (-0.093659) which confirms that the surface is planar and the valleys are more predominant [31]. S_{sk} also indicates the load carrying capacity and porosity of the material and the negative skewness is a criterion for a good bearing surface [32].

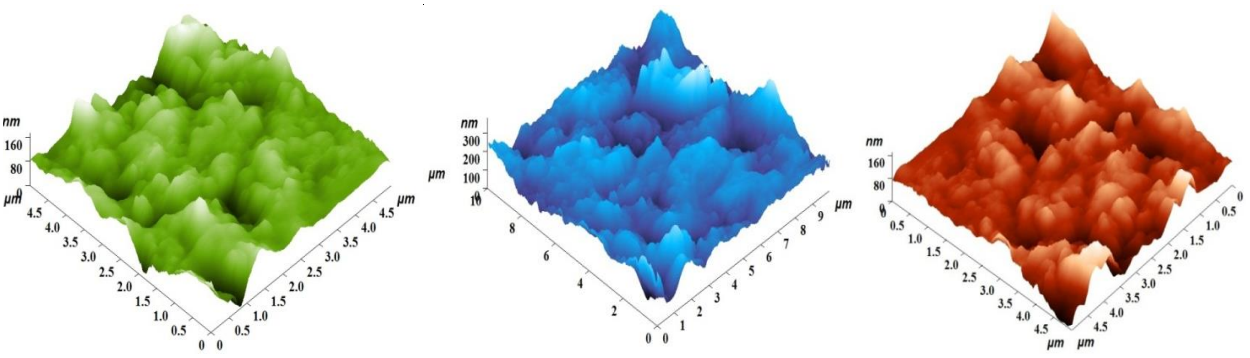

Figure 11 AFM images of BTCA crystal

The difference in height between the average of the five highest peaks and the five lowest valleys along the assessment length of the profile is termed as ten-point height (S_z) which is found to be 87.8115 nm for the grown crystal. Surface kurtosis (S_{ku}) is the measure of surface

sharpness and for BTCA crystal the S_{ku} is less than three which indicates that the surface is perfectly flat. From the study, it reveals the BTCA crystal has smooth and flat surface.

Table 2: Surface parameters measured by AFM

Parameter	BTCA
Roughness average (S_a)	17.2463 nm
Root mean square (S_q)	23.5593 nm
Surface skewness (S_{sk})	-0.093659
Surface kurtosis (S_{ku})	1.30554
Ten-point height (S_z)	87.8115nm

4. CONCLUSION

Semiorganic crystal of Bisthiourea Cadmium Acetate (BTCA) was synthesized by slow evaporation solution growth technique. The solubility studies reveal the crystal possesses positive gradient of solubility with good solubility in water. From the morphology studies it was observed that the growth along the 'b' axis is much higher than that of 'a' and 'c' axes. The powder diffraction confirms the perfection of good quality single crystal. In the PL spectrum a single broad emission peak was observed at 481 nm is the blue region confirms the structural perfection of the grown crystal. This confirms the suitability of BTCA crystal for optoelectronic and luminescence devices. Dielectric measurements show that dielectric constant and dielectric loss decreases with increase in frequency and the AC conductivity increases with frequency for different temperature which indicates BTCA is the potential material for NLO applications. Microhardness study shows that the hardness number H_v increases with increasing load exhibiting Reverse Indentation Size Effect. The value of Meyer's index, 'n' was found to be 4.43 and the grown crystal falls under the soft material category. The values of elastic stiffness

constant (C_{11}) indicates tight bonding between neighboring atoms. The SEM analysis reveals micro crystalline growth of the grown crystal. Atomic Force Microscopy analysis shows that the BTCA crystal possesses a smooth and flat surface.

ACKNOWLEDGEMENTS

The authors thank Dr. Babu Varghese and SAIF, IIT, Madras for conducting morphology and SEM studies respectively. The authors also thank Dr.N.Vijayan, NPL, Delhi and CNSNT, Sathyabama University for conducting Photoluminiscence and AFM studies.

REFERENCES

[1] G.Xing,M.Jiang, X.Zishao and D.Xu . J. Lasers. 14, 357 (1987)

[2] S.Versko.Laser Program Annual Report, Lawrence UCRC-JC 105000,Lawrence Livermore National Laboratory Livermore, CA. (1990)

[3] L.F.Warren. Electronic Materials our future in: R.E.Allred,R.J.Martinez.K.B.Wischmann . (Eds), Proceedings of the Foruth International Sample Electronics Society for the Advancement of Materials and Process Engineering Of Materials and Process Engineering, Covina. CA. 4,388 (1990)

[4] V. Venkataramanan, H. L. Bhat, M. R. Srinivasan,P. Ayyub And M. S. Multani, Journal of Raman Spectroscopy. 28, 779-784 (1997)

[5] S.S.Gupte, R.D.Pradhan,O.A.Mareano,N.Melikechi,C.F.Desai.J.Appl.Phys.91, 3125-3128 (2002)

[6] M.Jiang,Q. Fang. Adv. Mater. 11,1147-1151 (1999)

[7] P.M.Ushashree,R.Jayavel,C.Subramanium,P.Ramasamy. J.Crystal Growth. 197, 216-220 (1990)

[8]R.Rajasekaran,P.M.Ushashree,R. Jayavel,P. Ramasamy P. J.Crystal Growth. 229,563- 567 (2001)

[9]P.M.Ushashree,R.Muralidharan,R. Jayavel,P. Ramasamy. J.Crystal Growth. **218**, 365-371 (2000)

[10] V.Kannan,N.P.Rajesh,R.Bairava Ganesh,P.Ramasamy.J.Cryst Growth. 269, 565-569 (2004)

[11]S. Selvakumar, S.M.Ravi Kumar,K. Rajarajan,A.Joseph Arul Pragasam,S.A. Rajasekar, K.Thamizharasan,P.Sagayaraj.Cryst Growth Des. 6, 2607-2610 (2006)

[12]J.Uma,V. Rajendran. International Journal of Computer Applications. 30, 8-10 (2011)

[13] J.X.Wang,S.S. Xie,H.J.Yuan,X.Q.Yan,D.F.Liu,Y.Gao,Z.P.Zhou,L.Song,L.F.Liu,X.W.Zhao, X.Y.Dou,W.Y.Zhou,G.Wang, Solid State Commun, 131,435–440 (2004)

[14] S.M. Dharmaprakash, P. Mohan Rao, J. Mater. Sci. Lett. 8, 1167 (1989)

[15]S.A.Martin Britto Dhas,G.Bhagavannarayana and S.Natarajan. The Open Crystallography Journal.1,42-45 (2008)

[16] C.Miller. Appl phys Lett. 5, 17-19(1964)

[17] C.Balarew,R.Duhlew. J Solid state Chemistry. 55,1-6 (1984)

[18]M.R.Jagadeesh,H.M.Suresh Kumar and R.Ananda Kumari. Archives of Applied Science Research. 6,188-197 (2014)

[19]B. Uma , Rajnikant, K.Sakthi Murugesan,S. Krishnan,B.MiltonBoaz. Progress in Natural Science: Materials International. 24,378–387 (2014)

[20] K.Sangwal.Mater Chem Phys. 63,145-152 (2000)

[21] B.Basu, Mukhopadhyay,N.K.Manisha. J Eur Ceram Soc. 29,801-811(2009)

[22] P.Feltham,R.Banerjee. Journal Mater Sci. 27,1626-1632 (1992)

[23] M.Senthil Pandian,N. Balamurugan,G. Bhagavannarayana,P. Ramasamy. J Cryst Growth. 310,4143– 4147 (2008)

[24] E.Meyer. Z ver Dtsch Ing. 52, 645-654 (1908)

[25] E.M.Onitsch. Microskopie. 2, 131-151 (1947)

[26] M.Hanneman. Metall Manchu. 23,135-140 (1941)

[27] W.A.Wooster. Reports on Progress in Physics. 16, 62-82 (1953)

[28] J.R.CahoonW.H.Broughton and A.R.Kutzak.Metallurgical Transactions. 2,1979-1983 (1971)

[29] P.Saritha,S.Barathan,G.Sivakumar. IOSR Journal of Applied Physics (IOSR-JAP). 4, 38-41 (2013)

[30] M.Raposo,Q.Ferreia,P.A. Ribeiro. Modern research and educational topics in Microscopy, in:A.Mendz-Vilas,J.Diaz (Eds.),Micorscopic Book Series,Formatex,758 (2007)

[31]T.Rajesh Kumar,R.Jeyasekaran,S.M.Ravi Kumar,M.Vimalan and P. Sagayaraj. Appl. Surf. Sci. 257,1684–1691 (2010)

[32] B.Rajesh Kumar,T.Subba Rao. Digest Journal of Nanomaterials and Biostructures. 7,1881-1889 (2012)